

Price Volatility in Electricity Markets: A Stochastic Control Perspective*

Avi Mohan^{†1}, Shie Mannor^{‡1} and Arman Kizilkale^{§2}

¹Faculty of Electrical Engineering, Technion, Israel Institute of Technology

²Automai.ai

Abstract

Spot prices in deregulated electricity markets in the United States and Europe have historically displayed high volatility, leading to loss of revenue in high electricity costs, weakening economic growth and lost business from long blackouts. With rapidly increasing supply of intermittent solar and wind-based power, conditions in the foreseeable future are only expected to deteriorate. Geographic price variations, while capable of being quite dramatic themselves, are a natural outcome of Locational Marginal Pricing (LMP) that takes finite transmission capacity and congestion into consideration, to produce localized electricity prices. Temporal price volatility (considerable fluctuation over periods as short as an hour in particular), however, is harder to explain.

In an effort to unearth the cause of these price fluctuations, we propose to model the electricity market as a discrete time controlled stochastic process. While this is a stylized model, it facilitates the analysis of spot markets and helps exclude extraneous details that do not contribute significantly to the discussion. We show that in *any* such market, improving social welfare must necessarily be traded off with volatility in prices, i.e., it is impossible to reduce volatility in the price of electricity without sacrificing social welfare.

We also show that, akin to communication systems, every market has a *Capacity Region* associated with it, that dictates and quantifies how much welfare is achievable at a given level of price volatility. In the context of renewable power sources, our investigation uncovers an intriguing phenomenon we term the *volatility cliff*, which suggests that with increasing penetration of intermittent renewable production, price volatility could increase to unacceptable levels, prompting the need for a complete restructuring of existing electricity markets.

Index terms— Markets with friction, stochastic control, smart grids, constrained Markov decision processes, price volatility, renewable energy, spot pricing, real time markets.

1 Introduction

The deregulated electricity market in the United States is managed by two types of profit-neutral entities called Independent System Operators (ISOs) and Regional Transmission Organizations (RTOs). These

*Under review for SIGMETRICS 2020. Please do not distribute.

[†]avinashmohan@campus.technion.ac.il

[‡]shie@ee.technion.ac.il

[§]arman@automat.ai

entities are primarily responsible for the reliability of the power grid, resource planning i.e., keeping the power grid balanced between generation (supply) and load (demand), and determining electricity prices which, in turn, heavily influence supply, demand and future investment in the power sector. In fact, there is general consensus that setting real-time prices that reflect current operating conditions has multiple positive effects on the market such as the potential to reduce supplier ancillary cost and improving system efficiency [DoE06]. Consequently, the price of electricity, which we shall also refer to as the price *signal*, has assumed critical importance in wholesale power markets [Hog10].

However, in the years following the deregulation of the electricity market, volatile electricity prices have turned into an epidemic showing jumps of up to 300% over periods as short as one hour [gro15], and this phenomenon has been highlighted by researchers as a *feature* of the market [CM10, BMPV02, Rob05, KM10] rather than due to isolated cases of exercise of market power such as that involving the Enron Corporation [Fox03]. European markets, as seen in Fig. 1, have been experiencing similar fluctuations in prices. Additionally, accounting for transmission constraints across the grid and demand uncertainty localization has resulted in sharp geographical price variations. This mechanism, called *Locational Marginal Pricing* (LMP) can result in dramatic disparities in electricity prices such as in June 2010, when the price across a single RTO (the Pennsylvania, Jersey, Maryland Power Pool or PJM) varied by 635.65% [Ore].

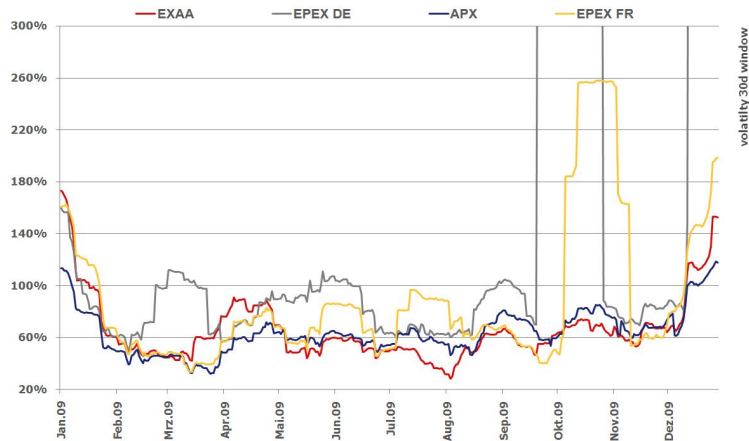


Figure 1: Market volatility of electricity prices in European power markets in 2009. The figure compares prices in four electricity exchanges namely, the Austrian energy exchange (red), European power exchange (EPEX) Germany (gray), EPEX France (yellow) and the APX group (blue). Of particular interest is the EPEX Germany price curve that fluctuates much more than 300% in Oct 2009 alone. Source: Wikimedia Commons [fEA].

Widespread adoption of “green” renewable energy sources such as windmills and photovoltaic (PV) cells is beginning to exacerbate this problem and has even led to long periods of *negative* electricity prices [Goe, ale], with suppliers paying to keep their generation plants running. Fig. 2 illustrates the infamous “duck curve” that regularly occurs in locations such as within the California ISO, where a substantial amount of solar electric capacity has been installed [DOBJ15]. Following periods of high solar generation during daytime, power suppliers need to rapidly increase their output using conventional sources (such as natural gas) around sunset to compensate for the sudden fall in solar power levels. This precipitous increase in demand only adds to the fluctuations in electricity prices. While improvements in grid energy storage technologies such as battery storage, pumped storage hydroelectricity and compressed air look promising, they suffer from multiple limitations such as prohibitively high investment costs, efficiency, need for appropriate geography, environmental impacts etc., and do not appear to be capable of solving the volatility problem at least in the near future [Wik19c, YJ11, Wik19a]. It is notable that, since the late 1990s, all these price variations

have resulted in an estimated \$45 billion in lost business from long blackouts, higher electricity costs and weakening economic growth in California alone [Rob05].

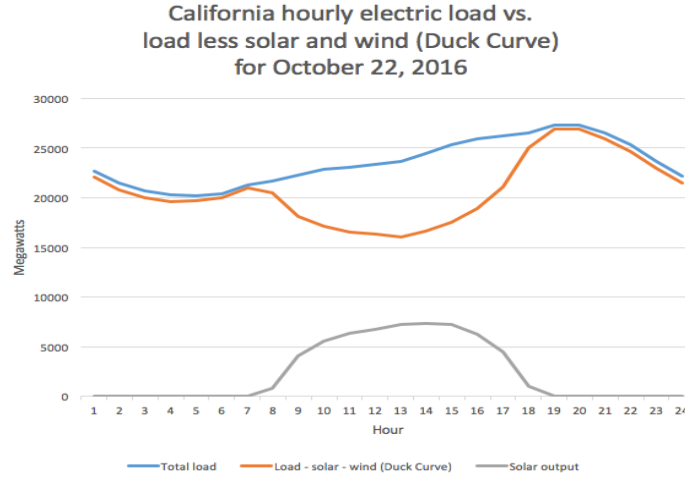


Figure 2: The infamous California ISO “Duck curve.” The orange plot represents the aggregate power generated over a period of 24 hours by renewable sources (wind and solar), while the blue plot represents the total demand on the system. The gray curve at the bottom shows the contribution from solar power sources. As renewable sources proliferate, this effect is expected to only worsen, as evidenced by states such as Hawaii, where a more pronounced version of this phenomenon, called the “Nessie curve” has been observed [Joh]. Source: Wikimedia Commons [Rei].

Analysis of this volatility phenomenon has received some attention in recent times. The work in [CM10, KM10] considered continuous time markets with friction, i.e., bounded rate of change of generation and/or demand, and showed that the optimal price signal, while not harming (a suitably defined notion of) social utility¹, does tend to fluctuate widely. The former article accounts only for supply-side friction and demonstrates using a stylized model, that the utility optimizing price tends to show extreme fluctuations in time. The latter expands this model to include demand-side friction in a market with Brownian activation, and demonstrates a similar result. [KM10] also shows a tradeoff between social utility and price volatility for this optimal market price process.

Two points are of interest here. Firstly, RTOs and ISOs run electricity markets at a minimum temporal granularity of about 5-15 minutes [RDM12, YO16]. This means that generation, demand and prices, even in real-time markets, are reevaluated only every 5-15 minutes². These markets, therefore, are not modeled well with continuous time dynamics and require a discrete time model for analysis. But this immediately renders the proof techniques in the aforementioned work unusable and we, in the current article, develop entirely new analytical machinery specifically for markets that operate in discrete time. Secondly, neither of these articles comments about the volatility behavior of other pricing policies. In the present article, we go further and show that volatility and social utility necessarily have to be traded off regardless of what pricing policy is used. We also completely characterize the space of (volatility, utility) tuples achievable in any given market. We hope that, akin to what the Shannon capacity region [CT12] did for communication systems, this result will help guide the development of pricing policies for such markets in general.

The electricity market is modeled as a *deterministic* discrete time dynamical system without supply-side friction in [RDM12]. The article analyzes social cost minimization under market clearing constraints, defines

¹We use the terms “social welfare” and “social utility” interchangeably.

²In fact, this is true in most regions of the United States such as New England, the PJM and California [RDM12]

a Lyapunov stability notion for the price process and derives conditions under which stability can be guaranteed. It also defines two notions of volatility: aggregate and time averaged, for price, demand and generation processes, and shows that when market dynamics satisfy certain smoothness assumptions, bounded volatility can be guaranteed. [WMO14] considers a deterministic finite time horizon (market closes after T time slots) market with a single supplier and multiple consumers. It defines a bounded quasilinear model of consumer utility (i.e., consumer i consumes at most d_i units over T slots), and derives a pricing mechanism to maximize social utility under an appropriately defined price fluctuation penalty. [WMO14] also provides a subgradient descent-based algorithm for implementing utility maximization in a decentralized manner. More recently, [SKX18] has adopted a game theoretic approach to solve this problem in the absence of the knowledge of consumer preferences (utility functions).

Turning to geographic price volatility, [YO16] adopts a stochastic control-based approach to analyze the impact of grid storage in mitigating sharp fluctuations in Locational Marginal Pricing (LMP). Increase in price variability due to widespread adoption of renewable sources could be observed as far back as 2011, when empirical studies analyzing spot-price variance using data from the Electricity Reliability Council of Texas (ERCOT) concluded that increased adoption of wind-based power sources tends to decrease spot prices on an average, but increases their temporal variability [WHMP11], i.e., prices tend to fluctuate more widely and faster. More recently, similar analysis of data from the California ISO also draws similar conclusions [Jos19].

1.1 Our contributions and organization

We now provide a road-map of the rest of the article together with a summary of our contributions.

- We begin with a model of the electricity market in Sec. 2. Our model is rich enough to capture the necessary market dynamics and demonstrate the price volatility effects we have described, and excludes extraneous details that might render it intractable without contributing significantly to the discussion. We define notions of “social cost,” “market efficiency” and “price volatility” that we analyze in depth in future sections of the paper. Assuming sufficient power transmission capacity, we ignore geographical price variations (i.e., Locational Marginal Pricing). and focus on temporal market evolution.
- We then study a tradeoff between the aforementioned market efficiency and volatility of market prices in Sec. 3. We prove that penalizing volatility in the optimal (in the sense of minimizing social cost) price process automatically penalizes market efficiency. We then provide a complete characterization of the set of all achievable (volatility, efficiency) tuples for any given market which we call its *capacity region*.
- Next, we analyze the effect of *decarbonization*, i.e., drastically increasing dependence on intermittent solar and wind generation, on price volatility (Sec. 4). Our study suggests the occurrence of a *volatility cliff* phenomenon which predicts that, with increasing penetration of intermittent renewable production, price fluctuation could increase to unacceptable levels. Echoing the assertions made in [Jos19] for renewed interest in electricity market reform, we hope that this result aids in convincing the reader of the need for a complete revamp of the existing electricity market structure to handle large-scale adoption of intermittent power sources.
- We then present simulations to help illustrate our results in Sec. 5. Finally, we provide concluding remarks and discuss possible directions for future work (Sec. 6).

2 Modeling energy market dynamics

RTOs and ISOs manage the power grid via two sub-markets: Day Ahead Markets and Real Time Markets that operate on time scales that range from 24 hours to 5 minutes. Electricity markets, therefore, are naturally amenable to being modeled as time-slotted systems. The state of the system under study at time $t \in \mathbf{N} = \{0, 1, \dots\}$, is described by the (demand, supply, price) tuple denoted by $\mathbf{x}_t = [d_t, s_t, p_t]^T$ and evolves in \mathbb{R}^3 according to the following law

$$\mathbf{x}_{t+1} = A\mathbf{x}_t + \mathbf{b}u_t + \mathbf{n}_t, t \in \mathbf{N}. \quad (\text{SYS})$$

We now proceed to explain the various elements of the above evolution equation. As is quite common in economic literature [CM10, KM10], the quantities d_t and s_t represent the aggregate of a continuum of infinitesimally small, identical consumers and energy suppliers. In the sequel, we deal with aggregate demand and supply. Here $u_t \in \mathbb{R}$ is the signal used to control the price of electricity in every time slot and $\mathbf{n}_t \in \mathbb{R}^3$ models random state disturbance. This ‘‘Linear Quadratic’’ control model has often been used to model markets with friction in general and electricity markets in particular in the literature [OMHU13, SKX18, KM10, BS89]. Taking into consideration standard facts in microeconomic theory that demand decreases with price and supply increases with price [MCWG⁺95], the matrix A is of the form ($\beta, \sigma, \phi_1, \phi_2$ below represent nonnegative reals)

$$A = \begin{bmatrix} \beta & 0 & -\phi_1 \\ 0 & \sigma & \phi_2 \\ 0 & 0 & 1 \end{bmatrix}, \quad (1)$$

$\mathbf{b} = [0, 0, 1]^T$, and the state disturbance $\{\mathbf{n}_t\}_{t \in \mathbf{N}}$ are IID random vectors drawn from some distribution F_n over \mathbb{R}^3 with $\mathbb{E}\mathbf{n}_t = \mathbf{0}$ and $\Psi_n := \mathbb{E}\mathbf{n}_t\mathbf{n}_t^T$. The regulatory authority (ISO or RTO) controls the price of electricity by tweaking the control input u_t in each time slot and the suppliers and consumers are coupled through this price. Therefore, u_t controls the rate of change of the price of electricity. Social utility is modeled through a single stage cost, defined by

$$g(\mathbf{x}_t, u_t) := \underbrace{\mathbf{x}_t^T Q \mathbf{x}_t}_{\text{state penalizing}} + \underbrace{r u_t^2}_{\text{control penalizing}}, \quad t \in \mathbf{N}, \quad (2)$$

where the matrix Q is assumed to be symmetric positive semidefinite (SPSD). Clearly, the first term in Eqn. 2 (i.e., $\mathbf{x}_t^T Q \mathbf{x}_t$) penalizes the state while the latter penalizes the control input u_t and, consequently, influences the rate at which price p_t varies with time. The control penalizing parameter (or control penalty coefficient) $r > 0$ in (2) will be of particular interest to us in subsequent sections. Given a discount factor $\gamma \in (0, 1)$, the problem to be solved by the regulatory authority now, is one of minimizing the γ -discounted cost defined by

$$\begin{aligned} J_r(\mathbf{x}_0) &:= \mathbb{E} \sum_{t=0}^{\infty} \gamma^t g(\mathbf{x}_t, u_t) \\ &= \mathbb{E} \sum_{t=0}^{\infty} \gamma^t (\mathbf{x}_t^T Q \mathbf{x}_t + r u_t^2), \end{aligned} \quad (3)$$

where the expectation is over both the state disturbance and the (possibly randomized) controls $\{u_t\}_{t=0}^{\infty}$. In (3), we have made explicit the fact that the cost functional $J_r(\cdot)$ depends on the control penalizing parameter r in anticipation of results to follow that will explore the impact of control penalization on various performance metrics. Note that the tuple (A, F_n, Q, r, γ) completely characterizes this market. We denote by $\mathcal{P}(\mathbb{R})$ the set of all probability distributions on \mathbb{R} .

For every $t \in \mathbb{N}$, let \mathcal{F}_t denote the sigma algebra generated by $\{\mathbf{x}_s, u_s, s < t\} \cup \{\mathbf{x}_t\}$. Throughout the article, we will only work with nonanticipatory controls, i.e., those that, at time t , use only the information available up to t and are of the form $u_t : \mathcal{F}_t \rightarrow \mathcal{P}(\mathbb{R})$. Restricting our attention to Markov controls, $u_t = \mu_t(\mathbf{x}_t)$, $t \in \mathbb{N}$, where $\mu_t : \mathbb{R}^3 \rightarrow \mathcal{P}(\mathbb{R})$ we define a **(Markov) policy** π to be a time indexed sequence of such maps $\pi = [\mu_0, \mu_1, \dots]$. If the constituent maps are independent of time, the policy is said to be **stationary**, in which case $\pi = [\mu, \mu, \dots]$. We denote by Π the set of all (nonanticipatory) policies for this system, by $\mathbb{F} \subset \Pi$ the set of all stationary policies and $\mathbb{D} \subset \mathbb{F}$, the set of all stationary **deterministic** policies.

The probability measure on the space of sample paths induced by policy π beginning in state \mathbf{x}_0 is denoted by $\mathbb{P}_{\mathbf{x}_0}^\pi$ and the associated expectation operator by $\mathbb{E}_{\mathbf{x}_0}^\pi$. The optimal cost functional is defined by

$$J_r^*(\mathbf{x}_0) := \inf_{\pi \in \Pi} \mathbb{E}_{\mathbf{x}_0}^\pi \sum_{t=0}^{\infty} \gamma^t (\mathbf{x}_t^T Q \mathbf{x}_t + r u_t^2). \quad (4)$$

Using Propositions 3.1.3 and 3.1.5 in [Ber11] we see that the optimal policy $\pi^* = [\mu^*, \mu^*, \dots]$ for this system is stationary and given by

$$u_t^* = \mu^*(\mathbf{x}) = -\gamma \frac{1}{\gamma \mathbf{b}^T K \mathbf{b} + r} \mathbf{b}^T K A \mathbf{x}, \quad (5)$$

where K is an SPSD matrix that satisfies the recursion

$$K = Q + A^T \left[\gamma K - \frac{1}{\gamma \mathbf{b}^T K \mathbf{b} + r} \gamma^2 K \mathbf{b} \mathbf{b}^T K \right] A. \quad (6)$$

A unique solution to (6) exists (and is, in fact, *positive definite*) provided the pair (A, b) is controllable and the pair (A, C) is observable [Ber95, Prop. 4.1], where $C = \sqrt{\Lambda} M$ and Λ and M are diagonal and orthogonal matrices respectively such that $Q = M^T \Lambda M$. Observability is easily guaranteed by choosing Q to be positive definite, which can be ensured by minimally perturbing the chosen Q with a scaled identity matrix. To guarantee controllability, we note that one requires the matrix $C_0 = [b \ Ab \ A^2 b]$ to be full rank. In our case,

$$C_0 = \begin{bmatrix} 0 & \phi_1 & \phi_1(\beta + 1) \\ 0 & -\phi_2 & -\phi_2(\sigma + 1) \\ 1 & 1 & 1 \end{bmatrix}.$$

This matrix is full rank when $\beta \neq \sigma$, which is the case in practice, since demand and supply rarely decrease or increase at exactly the same rate. Therefore, for the rest of the paper we have

Assumption 2.1. The system (A, \mathbf{b}) is controllable and the pair (A, C) is observable.

Under Assumption 2.1, the optimal cost is given by

$$J_r^*(\mathbf{x}_0) = \mathbf{x}_0^T K \mathbf{x}_0 + \frac{\gamma}{1 - \gamma} \mathbb{E} \mathbf{n}^T K \mathbf{n}, \quad \forall \mathbf{x}_0 \in \mathbf{R}^3, \quad (7)$$

where $\mathbf{n} \sim F_n$, the state disturbance distribution.

Given any pricing policy $\pi := [u_0, u_1, \dots]$ for the above system, define the **Volatility** of a policy by

$$\mathcal{V}_{\mathbf{x}_0}(\pi) := \mathbb{E}_{\mathbf{x}_0}^\pi \sum_{t=0}^{\infty} \gamma^t u_t^2. \quad (8)$$

Also define **Market Efficiency** under π by

$$\mathcal{E}_{\mathbf{x}_0}(\pi) := -\mathbb{E}_{\mathbf{x}_0}^\pi \sum_{t=0}^{\infty} \gamma^t \mathbf{x}_t^T Q \mathbf{x}_t. \quad (9)$$

In this paper, we will treat $\mathcal{E}_{\mathbf{x}_0}(\cdot)$ as a notion of social welfare. This, therefore, is something the regulatory authority (RTO/ISO) must attempt to maximize using a suitable pricing mechanism. We will call a pricing policy $\pi \in \Pi$ *admissible* if it the cost and volatility functionals are well defined under π and denote by $\mathcal{A} \subset \Pi$ the subset of all admissible policies. Finally, we define a *Bellman Operator* as follows. Let $\mathcal{S} = \mathbb{R}^3 \times (0, \infty)$ and let $\mathcal{G} = \{v \mid v : \mathcal{S} \rightarrow \mathbb{R}\}$ be the space³ of all functionals on \mathcal{S} . The Bellman Operator $T : \mathcal{G} \rightarrow \mathcal{G}$ is given by

$$(Tv)(\mathbf{x}, r) := \mathbf{x}^T Q \mathbf{x} + \inf_{u \in \mathbb{R}} r u^2 + \gamma \mathbb{E}_{\mathbf{n}} v(A\mathbf{x} + \mathbf{b}u + \mathbf{n}, r). \quad (10)$$

Having constructed the requisite theoretical scaffolding we will now move on to deriving a formal relationship between price fluctuations and market efficiency. Please note that we have provided a [glossary](#) of notation for the convenience of the reader in Sec. 7.1 in the Appendix.

3 Market Efficiency vs Price Volatility

We begin this section with Thm. 3.1 wherein we show that the optimal cost function, J_r^* , satisfies two important properties. Aided by this result, we then show that there exists a fundamental tradeoff between the volatility and efficiency functionals defined in Eqns. (8) and (9) under the pricing policy π^* that achieves the optimal cost (4). Next, invoking Thm. 3.1, we show that there exists a fundamental relation between the market efficiency that a price control policy can achieve and the volatility it engenders in the market. We also characterize the set of all (volatility, efficiency) pairs that can be achieved by any admissible price control mechanism in a given market (A, F_n, Q, r, γ) .

This latter result is of practical importance since it can be used to inform RTOs and ISOs about the consequences of price control policy decisions on market efficiency. On the flip side, it is also useful to know in advance, how much price volatility one can expect while attempting to achieve a desired efficiency level. We now discuss two important properties of J_r^* .

Theorem 3.1. $J_r^*(\mathbf{x})$ is concave and nondecreasing in r . Specifically,

$$\begin{aligned} \frac{dJ_r^*(\mathbf{x})}{dr} &> 0, \text{ and} \\ \frac{d^2 J_r^*(\mathbf{x})}{dr^2} &\leq 0, \forall \mathbf{x} \in \mathbb{R}^3. \end{aligned} \quad (11)$$

PROOF. The proof proceeds in several steps. We first define a norm $\|\cdot\| : \mathcal{G} \rightarrow \mathbb{R}_+$ by

$$\|v\| := \sup_{\mathbf{y} \in \mathcal{S}} \frac{|v(\mathbf{y})|}{(\|\mathbf{y}\|_2 \vee 1)^2}, \quad (12)$$

and let $\mathcal{V} := \{v \in \mathcal{G} : \|v\| < \infty\}$. Clearly, $J_r^* \in \mathcal{V}$. This norm induces a metric $\rho : \mathcal{V} \times \mathcal{V} \rightarrow \mathbb{R}_+$ defined by $\rho(v, w) = \|v - w\|$. Before proceeding further we first note that

Lemma 3.2. (\mathcal{V}, ρ) is a complete metric space, and $v \in \mathcal{V} \Rightarrow Tv \in \mathcal{V}$, i.e., the Bellman operator preserves finiteness of $\|\cdot\|$.

PROOF. See Sec. 7.2 in the Appendix. □

Next, we characterize the subspace of all $v \in \mathcal{V}$ that are nondecreasing and concave.

³We use ‘‘space’’ instead of ‘‘set’’ because we will convert \mathcal{G} to a metric space shortly.

Lemma 3.3. Let $\mathcal{H} := \{v \in \mathcal{V} : v \text{ is concave nondecreasing}\}$. Then,

1. \mathcal{H} is a closed subset of \mathcal{V} , where closure is in the topology induced by ρ , and
2. $v \in \mathcal{H} \Rightarrow Tv \in \mathcal{H}$.

PROOF. See Sec. 7.3 in the Appendix. □

We now note that (1) the function $v_0(\mathbf{y}) := 0, \forall \mathbf{y} \in \mathcal{S}$ is in \mathcal{H} , (2) that J^* is a fixed point of the operator T and observe the following

Lemma 3.4. $\lim_{k \rightarrow \infty} T^k v_0 = J^*$, where convergence is in the topology induced by ρ .

PROOF. See Sec. 7.4 in the Appendix. □

The above lemma, together with the fact that \mathcal{H} is closed, means that $J^* \in \mathcal{H}$. Furthermore, it is evident that $r \mapsto J_r^*(\mathbf{x}) \in \mathcal{C}^2((0, \infty))$ whence we have (11). This concludes the proof. □

The simulation result in Fig. 4 shows the concavity of J_r^* for the market specified in Sec. 7.10. Now, Thm. 3.1 has several consequences. To begin with, we show in Sec. 3.1 that it implies a fundamental tradeoff between Efficiency and Volatility for policy π^* defined in (5). Specifically, we will now show that the efficiency functional with π^* , i.e., $\mathcal{E}_{\mathbf{x}_0}(\pi^*)$ decreases with decreasing volatility, which means that improving optimal market efficiency comes at the cost of increased price volatility. However, in Sec. 3.2 we go even further and prove a stronger claim that this volatility-efficiency tradeoff must be satisfied by every admissible price control policy.

3.1 The Volatility-Efficiency tradeoff

Recall that the first term in the single stage cost was called the *state penalizing* portion (see Eqn. (2)) and consider the impact of employing the policy given in (5) on this cost alone, i.e., on

$$J_{sp,r}(\mathbf{x}_0) := \mathbb{E} \sum_{t=0}^{\infty} \gamma^t \mathbf{x}_t^T Q \mathbf{x}_t = -\mathcal{E}_{\mathbf{x}_0}(\pi^*), \quad (13)$$

where the subscript *sp* stands for “state penalizing.” It can be shown that that (see Prop. 7.1 in the Appendix) this cost is given by

$$J_{sp,r}(\mathbf{x}_0) = \mathbf{x}_0^T S \mathbf{x}_0 + \frac{\gamma}{1-\gamma} \mathbf{E} \mathbf{n}^T S \mathbf{n}, \quad (14)$$

where S is an SPSD matrix that satisfies

$$\begin{aligned} S &= Q + \gamma \left(A^T \left[I - \gamma \frac{1}{\gamma \mathbf{b}^T K \mathbf{b} + r} K \mathbf{b} \mathbf{b}^T \right] \right. \\ &\quad \left. \times S \left[I - \gamma \frac{1}{\gamma \mathbf{b}^T K \mathbf{b} + r} \mathbf{b} \mathbf{b}^T K \right] A \right). \end{aligned} \quad (15)$$

Proposition 3.5. Under Assumption 2.1, a unique symmetric positive definite matrix satisfying (15) exists. Moreover, the sequence of matrices generated by

$$\begin{aligned} S_{t+1} &= Q + \gamma \left(A^T \left[I - \gamma \frac{1}{\gamma \mathbf{b}^T K \mathbf{b} + r} K \mathbf{b} \mathbf{b}^T \right] \right. \\ &\quad \left. \times S_t \left[I - \gamma \frac{1}{\gamma \mathbf{b}^T K \mathbf{b} + r} \mathbf{b} \mathbf{b}^T K \right] A \right). \end{aligned} \quad (16)$$

with S_0 set to any SPSD matrix, satisfies

$$\lim_{t \rightarrow \infty} \| S_t - S \|_F = 0, \quad (17)$$

where S is the solution of (15) and $\| M \|_F$ is the Frobenius norm of matrix M .

PROOF. We first show in Prop. 7.1 in the Appendix, that $J_{sp,r}$ satisfies a Bellman-like fixed point equation which then gives us (14). Thereafter, we modify a general technique used in the analysis of Riccati equations to first prove convergence in the Frobenius norm of (16) when initialized with $S_0 = [0]_{3 \times 3}$ and extend the result to S_0 being any arbitrary SPSD matrix. Finally we show that the limit point has to be unique. See Sec. 7.6 in the Appendix for details. \square

Returning to (14), we now show that similar to our original cost functional J_r^* , the state penalizing functional is also concave nondecreasing in r , that is

Theorem 3.6 (V-E tradeoff). $J_{sp,r}(\mathbf{x})$ is concave nondecreasing in r . Specifically,

$$\begin{aligned} \frac{dJ_{sp,r}(\mathbf{x})}{dr} &> 0, \text{ and} \\ \frac{d^2J_{sp,r}(\mathbf{x})}{dr^2} &\leq 0, \forall \mathbf{x} \in \mathbb{R}^3. \end{aligned} \quad (18)$$

PROOF. The proof uses the ideas in the proof of Thm. 3.1, along with the fact that beginning with any SPSD matrix, the iterates in (16) converge in the Frobenius norm. Details can be found in Sec. 7.7 in the Appendix. \square

Since state penalizing cost is defined to be the negative efficiency in Eqn. (13), Thm. 3.6 shows that efficiency increases with increasing volatility, establishing the volatility-efficiency tradeoff. We thus see that operating an electricity market at high efficiency automatically entails highly volatile prices. The simulation results presented in Sec.5 illustrate this phenomenon very clearly.

3.2 The Capacity Region for Markets with Friction and A ‘‘No Free Lunch’’ theorem

Suppose we impose upon the stochastic control problem described in Sec. 2, the constraint that the volatility of the control law must not exceed a certain threshold $\alpha > 0$, i.e., that

$$V_{\mathbf{x}_0}(\pi) = \mathbb{E}_{\mathbf{x}_0}^{\pi} \sum_{t=0}^{\infty} \gamma^t u_t^2 \leq \alpha, \forall \mathbf{x}_0 \in \mathbb{R}^3. \quad (19)$$

For a given level $\alpha > 0$, we define $\mathcal{A}_{\alpha} \subset \mathcal{A}$ to be the set of all policies whose volatility is less than α and call these policies *α -admissible*. The policy that attains maximum efficiency, if it exists, must satisfy

$$\begin{aligned} \arg \max_{\pi \in \Pi} & \quad -\mathbb{E}_{\mathbf{x}_0}^{\pi} \sum_{t=0}^{\infty} \gamma^t \mathbf{x}_t^T Q \mathbf{x}_t \\ \text{subject to} & \quad \mathbf{x}_{t+1} = A \mathbf{x}_t + \mathbf{b} u_t + \mathbf{n}_t, t \in \mathbb{N}, \text{ and} \\ & \quad \mathbb{E}_{\mathbf{x}_0}^{\pi} \sum_{t=0}^{\infty} \gamma^t u_t^2 \leq \alpha. \end{aligned} \quad (20)$$

Clearly, all feasible solutions to the above problem are α -admissible and hence, the optimizer always lies within \mathcal{A}_α . This problem can be recast in the form of a *constrained* Markov decision process [Alt99, LMHL03], and solved with the aid of the Lagrangian $\mathcal{L} : \Pi \times (0, \infty) \rightarrow \mathbb{R}$, defined by

$$\begin{aligned} \mathcal{L}(\pi, \lambda) &:= \mathbb{E}_{\mathbf{x}_0}^\pi \sum_{t=0}^{\infty} \gamma^t \mathbf{x}_t^T Q \mathbf{x}_t + \lambda \left(\mathbb{E}_{\mathbf{x}_0}^\pi \sum_{t=0}^{\infty} \gamma^t u_t^2 - \alpha \right) \\ &= \mathbb{E}_{\mathbf{x}_0}^\pi \sum_{t=0}^{\infty} \gamma^t (\mathbf{x}_t^T Q \mathbf{x}_t + \lambda u_t^2) - \lambda \alpha, \end{aligned} \quad (21)$$

where we deliberately suppress the dependence of \mathcal{L} on \mathbf{x}_0 for ease of exposition. Note that in (21) the Lagrangian represents a cost minimization problem rather than an efficiency maximization problem. So our aim now will be to *minimize* this Lagrangian. Invoking Theorems 4.2 and 4.4 in [LMHL03], we see that the optimal cost \mathcal{L}^* for this constrained problem is given by

$$\begin{aligned} \mathcal{L}^* &= \inf_{\pi \in \Pi} \sup_{\lambda \geq 0} \mathcal{L}(\pi, \lambda) = \sup_{\lambda \geq 0} \inf_{\pi \in \Pi} \mathcal{L}(\pi, \lambda) \\ &= \sup_{\lambda \geq 0} \left(\inf_{\pi \in \Pi} \mathbb{E}_{\mathbf{x}_0}^\pi \sum_{t=0}^{\infty} \gamma^t (\mathbf{x}_t^T Q \mathbf{x}_t + \lambda u_t^2) \right) - \lambda \alpha. \end{aligned} \quad (22)$$

We solve for \mathcal{L}^* using this last expression. Notice that keeping $\lambda \geq 0$ fixed and using (7), $\inf_{\pi \in \Pi} \mathcal{L}(\pi, \lambda) = \mathbf{x}_0 K_\lambda \mathbf{x}_0 + \frac{\gamma}{1-\gamma} \mathbb{E} \mathbf{n}^T K_\lambda \mathbf{n}$, $\forall \mathbf{x}_0 \in \mathbb{R}$, where

$$K_\lambda = Q + A^T \left[\gamma K - \frac{1}{\gamma \mathbf{b}^T K \mathbf{b} + \lambda} \gamma^2 K \mathbf{b} \mathbf{b}^T K \right] A. \quad (23)$$

This gives us $\mathcal{L}^* = \sup_{\lambda \geq 0} \mathbf{x}_0 K_\lambda \mathbf{x}_0 + \frac{\gamma}{1-\gamma} \mathbb{E} \mathbf{n}^T K_\lambda \mathbf{n} - \lambda \alpha$, where $\mathbf{n} \sim F_n$, the state disturbance distribution. At the optimal λ , we have $\mathbf{x}_0 \frac{dK_\lambda}{d\lambda} \mathbf{x}_0 + \frac{\gamma}{1-\gamma} \mathbb{E} \mathbf{n}^T \frac{dK_\lambda}{d\lambda} \mathbf{n} = \alpha$, but since $\frac{d^2 K_\lambda}{d\lambda^2} \leq 0$, as α decreases, i.e., as we demand lesser price volatility, the optimal value of λ increases which, as Thm. 3.1 shows, means that $\mathbf{x}_0 K_\lambda \mathbf{x}_0 + \frac{\gamma}{1-\gamma} \mathbb{E} \mathbf{n}^T K_\lambda \mathbf{n}$ increases which results in decreased market efficiency.

However, we can go even further and make a stronger claim. We have already shown that the optimal cost of the constrained MDP, \mathcal{L}^* , is nonincreasing in the price volatility α . Notice that the Lagrangian dual, i.e.,

$$\mathcal{L}^* = \sup_{\lambda \geq 0} \mathbf{x}_0 K_\lambda \mathbf{x}_0 + \frac{\gamma}{1-\gamma} \mathbb{E} \mathbf{n}^T K_\lambda \mathbf{n} - \lambda \alpha, \quad (24)$$

is convex in α . Therefore, optimal market efficiency $\mathcal{E}_{\mathbf{x}_0}^* = -\mathcal{L}^*$ is *concave* in the volatility level α (Fig. 9 helps validate this conclusion experimentally for a market whose specifications are provided in Sec. 7.10 in the Appendix). Since $\mathcal{E}_{\mathbf{x}_0}^*$ is the maximum achievable efficiency for any given α , any other α -admissible policy $\pi \in \mathcal{A}_\alpha$ will necessarily only achieve lower (or at the very least not higher) efficiency.

The foregoing arguments seem to suggest that higher efficiency levels cannot be attained by any policy without sacrificing price volatility. We now show that this intuition is correct. Consider the tuple $(V_{\mathbf{x}_0}(\pi), \mathcal{E}_{\mathbf{x}_0}(\pi))$ for every $\pi \in \mathcal{A}_\alpha$ and let

$$\mathcal{C}_\alpha := \{(V_{\mathbf{x}_0}(\pi), \mathcal{E}_{\mathbf{x}_0}(\pi)) : \pi \in \mathcal{A}_\alpha\}.$$

We then have the following “no free lunch” theorem.

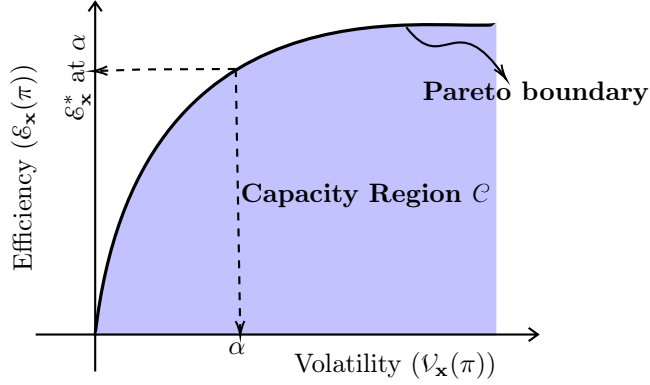


Figure 3: The Capacity Region of the market (A, F_n, Q, r, γ) . The Pareto boundary is the maximum efficiency, \mathcal{L}^* , of the constrained MDP (22). No (v, ε) pair outside \mathcal{C} is achievable in this market.

Theorem 3.7 (Market Capacity Region). For every market (A, F_n, Q, r, γ) , there exists a set $\mathcal{C} \subset \mathbb{R}^2$

$$\mathcal{C} = \bigcup_{\alpha > 0} \mathcal{C}_\alpha, \quad (25)$$

such that

- a. \mathcal{C} is closed and convex,
- b. the Pareto boundary of \mathcal{C} is given by the optimal efficiency $\varepsilon_{x_0}^*$, and
- c. for every $\pi \in \mathcal{A}$, the tuple $(V_{x_0}(\pi), \varepsilon_{x_0}(\pi)) \in \mathcal{C}$.

PROOF. The proof essentially involves showing that the set of all achievable (volatility, efficiency) tuples is contained in \mathcal{C} and later, that every point in \mathcal{C} is achievable. Details are presented in Sec. 7.8 in the Appendix. \square

Fig. 3 illustrates the set \mathcal{C} and the Pareto boundary for a market (A, F_n, Q, r, γ) . Since this region completely determines all achievable efficiencies under every acceptable level of price volatility, we call \mathcal{C} the **Capacity Region** of the market (A, F_n, Q, r, γ) , similar to the Shannon capacity region for the physical layer [CT12] and the Tassiulas-Ephremides capacity region for the MAC layer [TE90] of a communication system.

An example of such a region is shown in Fig. 9 in Sec. 5 for a particular market. This region is particularly useful for estimating an upper bound on the efficiency achievable both by different markets and by various pricing mechanisms for a given market. Price control policies are the outcome of decisions made within federal and local governments, and this analysis helps quantify the social impact such decisions entail. In general, these consequences are not very easy to judge off-hand. One recent example is the enormous price spike experienced by ERCOT where price capping and scarcity pricing policies lead to electricity being priced at \$9000/MWh and yet, defenders of the policy cited it as “a more efficient system” [Dap].

4 Effects of Decarbonization

In recent times, rejecting an incremental approach to solving climate change, undertakings such as the Deep Decarbonization Pathways Project (DDP) have focused on introducing drastic reductions in dependence on carbon-based fuel sources [Wik19b, PB16]. In Sec. 1, we outlined the deleterious effects that the entry of renewable energy sources can have on electricity prices. We now quantify the effects of endeavours such as the DDP on existing electricity markets using a modified system model, to incorporate these intermittent power sources and, in doing so, uncover a phenomenon we call a “volatility cliff.”

The output of a renewable energy source is highly dependent on ambient weather conditions. Solar power generation (even with controllable solar panels) is almost entirely at the mercy of the sun and local cloud cover. Similarly, windmills produce more power when the weather is windy. Taking this unique difficulty in controlling the output of these sources into consideration, we model renewable sources in the supply as a controlled random walk as follows

$$y_{t+1} = \sigma_r y_t + \sigma_c p_t + w_t, \quad t \geq 0. \quad (26)$$

Here, at time t , y_t is the aggregate output of installed renewable sources, p_t is the price control signal, w_t is the state disturbance and σ_r and σ_c are a positive constants. The price coefficient σ_c is a small positive constant used to model whatever rudimentary control the price signal can have over renewable supply. To incorporate this new evolution and keep the controlled process Markovian, we define the new system state vector to be $\mathbf{z}_t = [d_t, s_t, p_t, y_t]^T, t \geq 0$. We note that the state now evolves in \mathbb{R}^4 as opposed to the state in (SYS) that evolved in \mathbb{R}^3 . Therefore, the evolution equation (SYS) is modified to

$$\mathbf{z}_{t+1} = A_r \mathbf{z}_t + \mathbf{b}_r u_t + \mathbf{n}_t^{(r)}, \quad t \geq 0, \quad (\text{REN})$$

where

$$A_r = \begin{bmatrix} A & \mathbf{a}_r^{(1)} \\ (\mathbf{a}_r^{(2)})^T & \sigma_r \end{bmatrix}_{4 \times 4},$$

$\mathbf{b}_r = [0, 0, 1, 0]^T$, and the state disturbance $\mathbf{n}_t^{(r)} = [\mathbf{n}_t w_t]^T$ consists of IID random vectors with $\mathbb{E} \mathbf{n}_t^{(r)} = \mathbf{0}$ and $\mathbb{E} \mathbf{n}_t^{(r)} (\mathbf{n}_t^{(r)})^T = \Psi_n^{(r)}$. The vector $\mathbf{a}_r^{(1)} = [0, 1, 0]^T$, $\mathbf{a}_r^{(2)} = [0, 0, \sigma_c]^T$ and, assuming the state disturbance for supply, demand and renewables are independent of each other, the covariance matrix $\Psi_n^{(r)}$ is a diagonal matrix, with diagonal entries⁴ $[\psi_d, \psi_s, 0, \psi_r]$. Single stage cost is defined, as before, to be $g(\mathbf{z}_t, u_t) = \mathbf{z}_t^T Q \mathbf{z}_t + r u_t^2, t \geq 0$, and the cost functional $J_r^{(ren)}$ and efficiency $\mathcal{E}^{(ren)}$ are both defined as before, replacing \mathbf{x} with \mathbf{z} .

As renewable supplies proliferate (a) the aggregate supply from these sources obviously increases and (b) supplied power becomes more volatile. The factor in Eqn. (REN) that captures both of these effects is the renewable supply variance ψ_r . As the contribution of renewables increases, so does ψ_r . We then have the following result for the system (REN).

Proposition 4.1. Consider two renewable sources with supply variance $\psi_r^{(1)}$ and $\psi_r^{(2)}$. Also denote the price volatility of the system using renewable Source i by \mathcal{V}_i^* , $i = 1, 2$. Then, if $\psi_r^{(1)} < \psi_r^{(2)}$, $\mathcal{V}_1^* < \mathcal{V}_2^*$.

PROOF. See Sec. 7.9 in the Appendix. □

⁴We assume the price process is completely under the control of the regulatory authority and hence, doesn't have any noise in its evolution.

Prop. 4.1 leads us to conclude that as renewable energy sources become more widespread in the power grid, increased variability of prices in the *current* market structure is inevitable. This, then adds to the arguments presented in recent studies such as [Jos19] that call for a restructuring of the electricity market including and especially the pricing process.

In fact, as the result of simulating this system shows in Fig. 10, the effect is even more pernicious, in that increasing the fraction of renewable supply in the market causes the entire market capacity region to shrink. However, we reiterate that the results in this and the next section are not intended to stymie efforts towards decarbonization. Rather, they seek to highlight how the current market model might be insufficient to handle emerging green technologies such as wind and photovoltaic power supplies.

5 Numerical results

We now discuss the results of various simulation experiments conducted to support the theory we have developed in earlier sections. We begin with simulating the electricity market in (SYS). Details of the values of the market parameters used in the simulations are given in Sec. 7.10. Fig. 7 shows the effect of the control penalty coefficient r in (2). Two sample paths of the state of the market $x_t = [d_t, s_t, p_t]$ are shown with Fig. 5 demonstrating the effects of light control penalty ($r = 0.01$) and Fig. 6, the effects of heavy control penalty ($r = 10^3$). In both cases, we begin with the same initial condition $\mathbf{x}_0 = [25, 25, 50]$, but owing to the effect of the control penalty, the sample paths differ significantly in their evolution. When r is small, since large values of price control u_t are not penalized much, the price signal can be varied much more freely with the result that the market is more “stable,” in the sense that demand and supply do not fluctuate wildly over time.

The opposite is true in Fig. 6. When $r = 10^3$, the regulatory authority is highly constrained in the control that it can exercise upon the price signal and, consequently, the market is also less stable with demand and supply varying much more with time. For the sample paths in Fig. 6, the price volatility \mathcal{V} (defined in Eqn. 8) when $r = 0.01$ is 862.16, which is significantly larger than the volatility level of 0.07 obtained with $r = 10^3$. Thus, the experiment clearly shows that imposing a heavier control penalty (1) reduces price fluctuations, but (2) increases demand and supply volatility, which is essentially what Thm. 3.1 asserts.

Next, the simulation results shown in Fig. 4 help corroborate Thm. 3.1 and Thm. 3.6. Since the control input to the system is implicitly constrained while using large values of r , even though the control signal shows little volatility, both demand and supply show larger fluctuations, increasing the *state penalizing* portion in every time slot. Furthermore, comparing Equations (4) and (13) we see that the optimal cost function $J_r^*(\cdot)$ includes a non negative control penalty term in addition to the state penalty, which makes it the larger of the two metrics. As can be seen in the figure, both $J_r^*(\cdot)$ and the state penalizing cost function $J_{sp,r}(\cdot)$ are increasing and concave in the control penalty coefficient r .

Moving on to market capacity regions, for a given electricity market (A, F_n, Q, r, γ) , define for every price volatility level α , the function

$$q_\alpha(\lambda) = \mathbf{x}_0 K_\lambda \mathbf{x}_0 + \frac{\gamma}{1-\gamma} \mathbb{E} \mathbf{n}^T K_\lambda \mathbf{n} - \lambda \alpha. \quad (27)$$

We see that the optimal value of the constrained MDP $\mathcal{L}^* = \sup_{\lambda \geq 0} q_\alpha(\lambda)$ (see Eqns. (21) and (22)). The arguments presented in Sec. 3.2 and in Thm. 3.7 show that both $q_\alpha(\cdot)$ and \mathcal{L}^* are concave functions of λ and α respectively. Figures 8 and 9 show that this is indeed true.

Fig. 9 shows the capacity region associated with *two* markets with $\gamma = 0.5$ and $\gamma = 0.9$ respectively. For a given value of α , suppose that the optimal control with $\gamma = 0.9$ is $\left(u_t^{(0.9)}\right)_{t=0}^\infty$ and $\mathcal{L}_{0.9}^*$ is the optimal

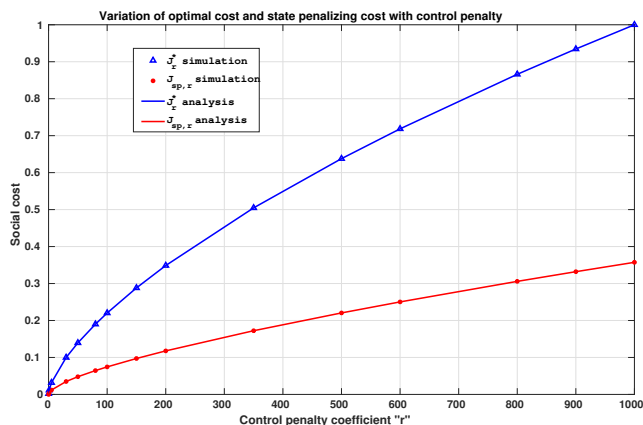


Figure 4: Variation of social cost as a function of the control penalty r under the optimal pricing policy π^* in (5). The plot shows that both the optimal cost J_r^* and the state penalizing cost $J_{sp,r}$ are concave and increasing in r . Note that both curves have been normalized to lie in $[0, 1]$.

cost. When this same control is used in a market with $\gamma = 0.5$ starting with the same initial conditions, the resulting sample paths are identical, but the cost only reduces, since γ has reduced. But since applying the optimal control $\left(u_t^{(0.5)}\right)_{t=0}^{\infty}$ can only further reduce cost, the efficiency with the latter discount factor must be larger, giving rise to a bigger capacity region. We see Fig. 9 bearing this out. Once again, the parameters (A, F_n, Q, r, γ) , specifying the markets upon which we have performed this simulation, are given in Sec. 7.10. Note that in Fig. 9, the maximum attainable efficiency curve $\mathcal{E}_{\mathbf{x}_0}^*$ has been normalized to peak at 1 for $\gamma = 0.5$. We also refer to this curve as the ‘‘Pareto Boundary’’ since no achievable vector can give strictly greater efficiency for a given level of volatility. The region below the $\mathcal{E}_{\mathbf{x}_0}^*$ curve, shaded blue and pink, are the capacity regions of the markets, i.e., every (V, \mathcal{E}) tuple in these regions is achievable by some admissible policy.

In Sec. 4 we described the deleterious effects that unchecked penetration of renewable energy sources can have on market efficiency and price volatility. Recall that in Prop. 4.1, we already argued why increasing renewable supply penetration (modeled by increasing ψ_r) results in higher price volatility. Here, we go further and present a simulation supporting a stronger claim. Let $\mathcal{C}^{(\psi_r)}$ denote the capacity region associated with renewables penetration level of $\psi_r = \mathbb{E}w_t^2$, where the latter is defined in (26). Fig. 10 illustrates precisely how quickly the achievable efficiency is lost when renewable sources increase in the current market structure. As seen in the figure, as ψ_r , the contribution of renewable sources, increases, the associated capacity regions shrink, with the loss in capacity becoming much more pronounced with increasing ψ_r . In the Supplementary Material, aided by a more realistic market model, we show a starker version of this result⁵ (see Sec. 8). These observations add to the increasing groundswell in support of fundamental restructuring of electricity markets to survive the imminent influx of green power generation technologies [Rob, Jos19].

6 Concluding remarks and Future Work

In this paper we presented an analysis of the time slotted real-time electricity market, with the aim to uncover the reasons for frequently observed sharp fluctuations in market prices. With the aid of a stylized

⁵We are unable to include this in the main text owing to space constraints.

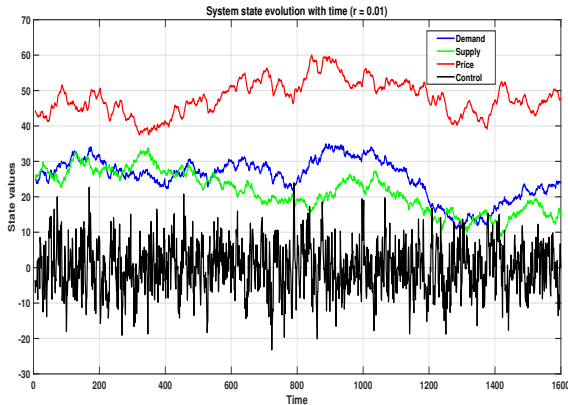


Figure 5: $r = 0.01$

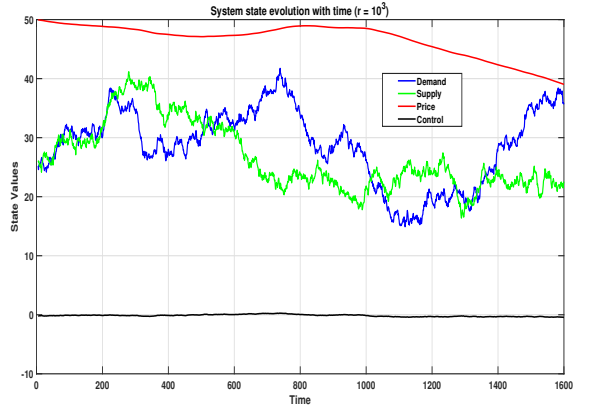


Figure 6: $r = 10^3$

Figure 7: State dynamics with varying control penalty coefficient r . In Fig. 5, the control penalty is small and variations in the price process $\{p_t, t \geq 0\}$ and control $\{u_t, t \geq 0\}$ are large, while in Fig. 6, since control fluctuations are being heavily penalized, price fluctuates less.

linear quadratic γ -discounted cost model, we showed that price volatility and social welfare are actually inextricably related in a natural tradeoff, where penalizing one is always to the detriment of the other.

We then proved that associated with every market, is a capacity region that dictates all (volatility, welfare) tuples that can possibly be achieved. We also showed that the entry of renewable sources into the market can harm price stability. Going into a renewables-rich future, we therefore need a firm theoretical scaffolding to help construct a new grid to cope with all these new phenomena.

In this article, we studied consumers and producers from a price-taking perspective and did not consider *strategic* market players. In most cases this is justifiable, since consumers generally are not interested in attempting to “game” the system by behaving strategically. Moreover, the *aggregate* demand and supply (that we work with) in a sufficiently large RTO/ISO could neutralize strategic effects and render the market immune to gaming. But in the absence of these factors, collusion and strategic behavior might have undesirable effects on the market. Therefore, in future work, we will address the issue of strategic consumers and suppliers by taking a more decentralized approach to the problem, modeling the market as a collection of multiple non-atomic/non-infinitesimal suppliers and consumers to provide a more nuanced analysis. In this framework, one could also consider network effects and study price fluctuations across both space (Locational Marginal Pricing) and time.

One technique proposed in [KDMT16] to handle increasing renewable supply penetration calls for a departure from what they term the “The Grand Central Optimization” (GCO) paradigm to a “Layered Decentralized Optimization” (LDO) paradigm. The former, GCO, refers to the existing electricity market structure where a centralized authority (RTO/ISO) is given all system information and takes all pricing and demand-supply balance decisions. It is argued in [KDMT16] that as the number of intermittent renewable sources (especially on the demand side) increases, gathering information about the entire state space in real time and optimizing over such a large state space might become infeasible. Therefore, a decentralized *tiered* architecture (LDO) with hierarchical decision-making entities is designed as an alternative. This new market needs to be analyzed in greater detail. Further, Dual Pricing is another option that as been explored in the literature, for example in [KM11], as a potential method to reduce price volatility.

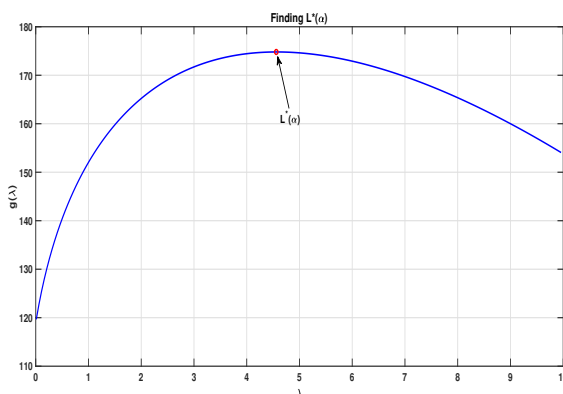


Figure 8: Illustrating the behavior of the function q_α , defined in Eqn. (27), for the market whose parameters are given in Sec. 7.10, at $\alpha = 27$. The function, as argued in Sec. 3.2, is *concave* in λ . The value of the constrained MDP for a given acceptable volatility level α , $L^*(\alpha) = \sup_{\lambda \geq 0} q_\alpha(\lambda)$, is also shown in the figure.

References

- [ale] Wind energy caused negative prices in germany and will lower the markets' prices this week.
- [Alt99] Eitan Altman. *Constrained Markov decision processes*, volume 7. CRC Press, 1999.
- [Ber95] Dimitri P Bertsekas. *Dynamic programming and optimal control*, volume 1. Athena scientific Belmont, MA, 1995.
- [Ber11] Dimitri P Bertsekas. Dynamic programming and optimal control 3rd edition, volume ii. *Belmont, MA: Athena Scientific*, 2011.
- [BMPV02] Michele Benini, Mirko Marracci, Paolo Pelacchi, and Andrea Venturini. Day-ahead market price volatility analysis in deregulated electricity markets. In *IEEE Power Engineering Society Summer Meeting.*, volume 3, pages 1354–1359. IEEE, 2002.
- [BN03] Dimitri Bertsekas and Angelia Nedic. *Convex analysis and optimization*. 2003.
- [BS89] Arthur W Berger and Fred C Schweppe. Real time pricing to assist in load frequency control. *IEEE Transactions on Power Systems*, 4(3):920–926, 1989.
- [CM10] In-Koo Cho and Sean P Meyn. Efficiency and marginal cost pricing in dynamic competitive markets with friction. *Theoretical Economics*, 5(2):215–239, 2010.
- [CT12] Thomas M Cover and Joy A Thomas. *Elements of information theory*. John Wiley & Sons, 2012.
- [Dap] Matt Daprato. Texas' power price spike and designing markets for a carbon-free grid.
- [DOBJ15] Paul Denholm, Matthew O'Connell, Gregory Brinkman, and Jennie Jorgenson. Overgeneration from solar energy in california. a field guide to the duck chart. Technical report, National Renewable Energy Lab.(NREL), Golden, CO (United States), 2015.
- [DoE06] US DoE. Benefits of demand response in electricity markets and recommendations for achieving them. a report to the united states congress pursuant to section 1252 of the energy policy act of 2005. In *US Washington, DC: Department of Energy.[http://eetd. lbl.gov/ea/EMP/reports/congress-1252d. pdf](26 July 2009)*, 2006.

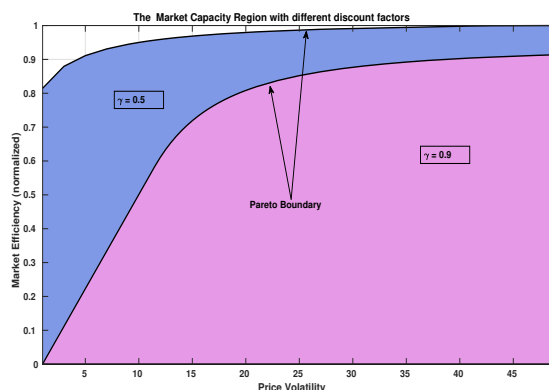


Figure 9: The capacity regions with discount factor $\gamma = 0.5$ and $\gamma = 0.9$ (normalized to peak at 1 with $\gamma = 0.5$) for the markets whose parameters (A, F_n, Q) are given in Sec. 7.10. The control penalty is set to $r = 0.01$. The Pareto boundary is defined by the optimal volatility function ε^* . The regions below these boundaries, shaded blue and pink, are the capacity regions with $\gamma = 0.5$ and $\gamma = 0.9$ respectively.

- [fEA] EXAA Abwicklungsstelle für Energieprodukte AG. File:volatility electricity price 2009.jpg.
- [Fox03] Loren Fox. *Enron: The rise and fall*. John Wiley and Sons, 2003.
- [Goe] Philipp Goetz. Already 103 times “negative electricity prices” at the spot market.
- [gro15] Solomon Energy group. Why are electricity prices so volatile? 2015.
- [HJ12] Roger A Horn and Charles R Johnson. *Matrix analysis*. Cambridge university press, 2012.
- [Hog10] William W Hogan. Demand response compensation, net benefits and cost allocation: comments. *The Electricity Journal*, 23(9):19–24, 2010.
- [ISO] The California ISO.
- [Joh] Jeff St. John. Hawaii’s solar-grid landscape and the “Nessie Curve”.
- [Jos19] Paul L Joskow. Challenges for wholesale electricity markets with intermittent renewable generation at scale: the us experience. *Oxford Review of Economic Policy*, 35(2):291–331, 2019.
- [KDMT16] Lorenzo Kristov, Paul De Martini, and Jeffrey D Taft. A tale of two visions: Designing a decentralized transactive electric system. *IEEE Power and Energy Magazine*, 14(3):63–69, 2016.
- [KM10] Arman C Kizilkale and Shie Mannor. Regulation and efficiency in markets with friction. In *49th IEEE Conference on Decision and Control (CDC)*, pages 4137–4144. IEEE, 2010.
- [KM11] Arman C Kizilkale and Shie Mannor. Regulation and double price mechanisms in markets with friction. In *2011 50th IEEE Conference on Decision and Control and European Control Conference*, pages 33–40. IEEE, 2011.
- [KR00] Thomas Klitgaard and Rekha Reddy. Lowering electricity prices through deregulation. *Current Issues in Economics and Finance*, 6(14), 2000.

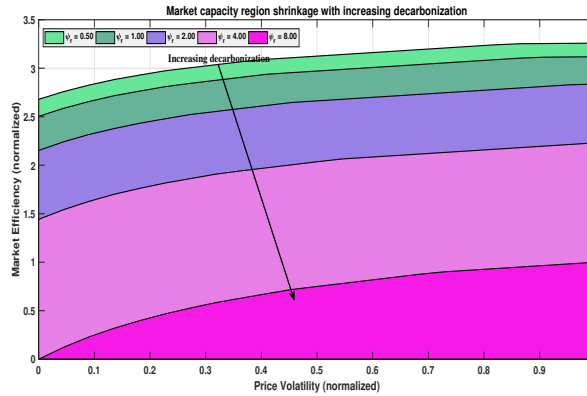


Figure 10: The capacity region for the market (A, F_n, Q, r, γ) shrinks as renewables penetrate the market. We see that as ψ_r , the renewable source contribution to the market increases from 0.5 to 8.0, the capacity region shrinks slowly at first, but rapidly thereafter, until around $\psi_r = 8.0$, barely any of the original efficiency (i.e., in $C^{(0.5)}$) is achievable. The regions have been normalized such that $C^{(8.0)}$ peaks at 1.

- [LMHL03] Raquel R López-Martínez and Onésimo Hernández-Lerma. The lagrange approach to constrained markov control processes: A survey and extension of results. *Morfismos*, 7(1):1–26, 2003.
- [MCWG⁺95] Andreu Mas-Colell, Michael Dennis Whinston, Jerry R Green, et al. *Microeconomic theory*, volume 1. Oxford university press New York, 1995.
- [OMHU13] Yusuke Okajima, Toshiyuki Muraio, Kenji Hirata, and Kenko Uchida. A dynamic mechanism for lqg power networks with random type parameters and pricing delay. In *52nd IEEE Conference on Decision and Control*, pages 2384–2390. IEEE, 2013.
- [Ore] Shmuel Oren. A primer to competitive electricity markets: Smart markets for a smart grid.
- [PB16] Steve Pye and Chris Bataille. Improving deep decarbonization modelling capacity for developed and developing country contexts. *Climate Policy*, 16(sup1):S27–S46, 2016.
- [RDM12] Mardavij Roozbehani, Munther A Dahleh, and Sanjoy K Mitter. Volatility of power grids under real-time pricing. *IEEE Transactions on Power Systems*, 27(4):1926–1940, 2012.
- [Rei] Arnold Reinhold. File:duck curve ca-iso 2016-10-22.agr.png.
- [Rob] David Roberts. Clean energy technologies threaten to overwhelm the grid. here’s how it can adapt.
- [Rob05] Sara Robinson. Math model explains high prices in electricity markets. *Siam News*, 38(7):8–10, 2005.
- [SKX18] Rahul Singh, PR Kumar, and Le Xie. Decentralized control via dynamic stochastic prices: The independent system operator problem. *IEEE Transactions on Automatic Control*, 63(10):3206–3220, 2018.
- [TE90] Leandros Tassiulas and Anthony Ephremides. Stability properties of constrained queueing systems and scheduling policies for maximum throughput in multihop radio networks. In *29th IEEE Conference on Decision and Control*, pages 2130–2132. IEEE, 1990.

- [WHMP11] Chi-Keung Woo, Ira Horowitz, Jack Moore, and Andres Pacheco. The impact of wind generation on the electricity spot-market price level and variance: The texas experience. *Energy Policy*, 39(7):3939–3944, 2011.
- [Wik19a] Wikipedia contributors. Compressed-air energy storage — Wikipedia, the free encyclopedia. https://en.wikipedia.org/w/index.php?title=Compressed-air_energy_storage&oldid=931654698, 2019. [Online; accessed 12-January-2020].
- [Wik19b] Wikipedia contributors. Deep decarbonization pathways project — Wikipedia, the free encyclopedia. https://en.wikipedia.org/w/index.php?title=Deep_Decarbonization_Pathways_Project&oldid=916027085, 2019. [Online; accessed 13-January-2020].
- [Wik19c] Wikipedia contributors. Pumped-storage hydroelectricity — Wikipedia, the free encyclopedia. https://en.wikipedia.org/w/index.php?title=Pumped-storage_hydroelectricity&oldid=930517435, 2019. [Online; accessed 12-January-2020].
- [WMO14] E. Wei, A. Malekian, and A. Ozdaglar. Competitive equilibrium in electricity markets with heterogeneous users and price fluctuation penalty. In *53rd IEEE Conference on Decision and Control*, pages 6452–6458, Dec 2014.
- [YJ11] Chi-Jen Yang and Robert B Jackson. Opportunities and barriers to pumped-hydro energy storage in the united states. *Renewable and Sustainable Energy Reviews*, 15(1):839–844, 2011.
- [YO16] Insoon Yang and Asuman E Ozdaglar. Reducing electricity price volatility via stochastic storage control. In *2016 American Control Conference (ACC)*, pages 4138–4144. IEEE, 2016.

7 Appendix

7.1 Glossary of Notation

- $\mathbf{x} = [d, s, p]$: the state space of the discrete time market model. comprising demand, supply and price, respectively.
- $\mathbb{N} = \mathbb{N} \cup \{0\} = \{0, 1, 2, \dots\}$ the set of natural numbers including 0.
- A : the gain matrix in the state evolution equation (SYS) relating current state to the state in the next time step.
- \mathbf{b} : the coefficient of the price control input in (SYS).
- \mathbf{n} : the state disturbance process.
- F_n : the probability distribution function of \mathbf{n} .
- Ψ_n : the covariance matrix of \mathbf{n} .
- γ : the discount factor in the Markov decision process formulation (3), $\gamma \in (0, 1)$.
- r : control volatility penalty.
- (A, F_n, Q, r, γ) : a market is fully determined by this tuple.
- Π : the set of all nonanticipatory policies.
- F : the set of all Markov policies.
- D : the set of all deterministic Markov policies.
- \mathcal{A} : the set of all admissible policies. Admissibility is defined towards the end of Sec. 2.
- $\mathbb{P}_{\mathbf{x}}^{\pi}$: the probability measure induced by policy π on the space of all sample paths, when the initial state of the system is \mathbf{x} .
- $\mathbb{E}_{\mathbf{x}}^{\pi}$: the expectation operator associated with $\mathbb{P}_{\mathbf{x}}^{\pi}$.
- $\mathcal{P}(\mathbb{R})$: the set of all probability distributions on \mathbb{R} .
- J_r^* : the optimal cost functional for a given value of r .
- $\mathcal{V}_{\mathbf{x}}(\pi)$: the volatility of the price process under policy π when the initial state of the system is \mathbf{x} defined in (8)
- $\mathcal{E}_{\mathbf{x}}(\pi)$: the efficiency achieved by the price process under policy π when the initial state of the system is \mathbf{x} , defined in (9).
- $\mathcal{S} = \mathbb{R}^3 \times (0, \infty)$
- T : the Bellman operator defined in (10).
- $J_{sp,r}$: the state penalizing cost defined in (13).
- \mathcal{C} : the capacity region of the market (A, F_n, Q, r, γ) .

7.2 Proof of Lem. 3.2

First note that convergence in $\|\cdot\|$ implies pointwise convergence. Let v be a limit point of \mathcal{V} . Therefore, there exists a sequence $v_k, k \geq 0$ in \mathcal{V} such that $\lim_{k \rightarrow \infty} \|v - v_k\| = 0$. But this implies that $\|v\| \leq \|v - v_k\| + \|v_k\| < \infty$. Hence, $v \in \mathcal{V}$. Moreover, $v \in \mathcal{V} \Rightarrow Tv \in \mathcal{V}$, since

$$\begin{aligned} (Tv)(\mathbf{x}, r) &= \mathbf{x}^T Q \mathbf{x} + \inf_{u \in \mathbb{R}} r u^2 + \gamma \mathbb{E}_{\mathbf{n}} v(A\mathbf{x} + \mathbf{b}u + \mathbf{n}, r) \\ &\leq \mathbf{x}^T Q \mathbf{x} + \inf_{u \in \mathbb{R}} r u^2 \\ &\quad + \gamma \mathbb{E}_{\mathbf{n}} \|(A\mathbf{x} + \mathbf{b}u + \mathbf{n})\|^2 + r^2 + 1 \end{aligned} \tag{28}$$

The RHS of (28) is quadratic in (\mathbf{x}, r) and, hence, $\|Tv\| < \infty$. \square

7.3 Proof of Lem. 3.3

The closure of \mathcal{H} , i.e., that it contains all its limit points, follows immediately from the observation that convergence in $\|\cdot\|$ always implies pointwise convergence. Moving on to the next claim in the Lemma, observe that $\forall v \in \mathcal{H}$ and $(\mathbf{x}, r) \in \mathcal{S}$,

$$(Tv)(\mathbf{x}, r) = \mathbf{x}^T Q \mathbf{x} + \underbrace{\inf_{u \in \mathbb{R}} r u^2}_{\text{linear in } r} + \underbrace{\gamma \mathbb{E}_{\mathbf{n}} v(A\mathbf{x} + \mathbf{b}u + \mathbf{n}, r)}_{\text{concave in } r}.$$

Since Tv is the pointwise infimum of a collection of concave functions, it is itself concave in r . That Tv is non decreasing whenever v is, follows mutatis mutandis. \square

7.4 Proof of Lem. 3.4

It is easy to see that, starting with v_0 , the all zero function⁶, for $\forall t \geq 0$, and $\forall (\mathbf{x}, r) \in \mathcal{S}$,

$$T^{(t+1)}v_0(\mathbf{x}, r) = \mathbf{x}^T K_t \mathbf{x} + \sum_{m=0}^{t-1} \gamma^{k-m} \mathbb{E}_{\mathbf{n}}^T K_m \mathbf{n},$$

where, the matrices K_t are defined by

$$\begin{aligned} K_0 &= Q \\ K_{t+1} &= Q + A^T \left[\gamma K_t - \frac{1}{\gamma \mathbf{b}^T K_t \mathbf{b} + r} \gamma^2 K_t \mathbf{b} \mathbf{b}^T K_t \right] A, \quad t \geq 0. \end{aligned}$$

Also recall from Eqn. (7) that

$$J_r^*(\mathbf{x}) = \mathbf{x}^T K \mathbf{x} + \frac{\gamma}{1 - \gamma} \mathbb{E}_{\mathbf{n}}^T K \mathbf{n}, \quad \forall \mathbf{x} \in \mathbf{R}^3. \tag{29}$$

⁶Meaning $v_0(\mathbf{x}, r) = 0, \forall (\mathbf{x}, r) \in \mathcal{S}$.

Therefore,

$$\begin{aligned}
\left| T^{(t+1)}v_0(\mathbf{x}, r) - J_r^*(\mathbf{x}) \right| &= \left| \mathbf{x}^T(K_t - K)\mathbf{x} + \underbrace{\sum_{m=0}^{k-1} \gamma^{k-m} \mathbb{E} \mathbf{n}^T K_m \mathbf{n}}_{T1} \right. \\
&\quad \left. - \frac{\gamma}{1-\gamma} \mathbf{n}^T K_m \mathbf{n} \right| \\
&\leq \underbrace{\left| \mathbf{x}^T(K_t - K)\mathbf{x} \right|}_{T1} \\
&\quad + \underbrace{\left| \sum_{m=0}^{k-1} \gamma^{k-m} \mathbb{E} \mathbf{n}^T K_m \mathbf{n} - \frac{\gamma}{1-\gamma} \mathbf{n}^T K_m \mathbf{n} \right|}_{T2}.
\end{aligned}$$

Under observability and controllability, K_t converges pointwise to K [Ber95, Prop. 4.1]. So, coming to term $T1$ above, we see that

$$\lim_{t \rightarrow \infty} \sup_{(\mathbf{x}, r) \in \mathcal{S}} \frac{|\mathbf{x}^T(K_t - K)\mathbf{x}|}{(\|\mathbf{x}, r\|_2 \vee 1)} \leq \lim_{t \rightarrow \infty} \|K_t - K\|_F = 0, \quad (30)$$

where $\|A\|_F$ is the Frobenius norm of matrix A . Similarly, $T2$ vanishes as $t \rightarrow \infty$ due to the pointwise convergence of K_t to K . \square

7.5 State penalizing cost

Proposition 7.1. The γ -discounted cost of applying the stationary policy $\pi^* = [u_0^*, u_1^*, \dots]$ where $u_t^*(\mathbf{x}) = -\frac{1}{\mathbf{b}^T K \mathbf{b} + r} \mathbf{b}^T K \mathbf{A} \mathbf{x}$, to the system in Eqn. (SYS) with single-stage cost $g(\mathbf{x}_t, u_t) = x_t^T Q x_t, t \geq 0, \mathbf{x} \in \mathbb{R}^3$ is given by (15), i.e.,

$$J_{sp,r}(\mathbf{x}_0) = \mathbf{x}_0^T S \mathbf{x}_0 + \frac{\gamma}{1-\gamma} \mathbb{E} \mathbf{n}^T S \mathbf{n}, \quad (31)$$

where S satisfies

$$S = Q + \gamma A^T \left[I - \frac{1}{\mathbf{b}^T K \mathbf{b} + r} K \mathbf{b} \mathbf{b}^T \right] S \left[I - \frac{1}{\mathbf{b}^T K \mathbf{b} + r} \mathbf{b} \mathbf{b}^T K \right] A. \quad (32)$$

PROOF. The function $J_{sp,r}(\cdot)$ is, by definition, the γ -discounted cost of applying the stationary control $u_t^*(\mathbf{x}) = -\frac{1}{\mathbf{b}^T K \mathbf{b} + r} \mathbf{b}^T K \mathbf{A} \mathbf{x}$ to the system in (SYS). Computing $J_{sp,r}$, therefore, can be cast as applying π^* to a γ -discounted controlled Markov process, specified by

- State space: $\mathcal{S} = \mathbb{R}^3 \times (0, \infty)$
- Action space: $\mathbf{A} = \mathbb{R}$. Note that $U(\mathbf{x}, r) = \mathbb{R} \forall (\mathbf{x}, r) \in \mathcal{S}$.
- Transition probability kernel: Let $\mathcal{K} = \{(\mathbf{y}, u) \in \mathcal{S} \times \mathbf{A} \mid u \in U(\mathbf{y})\}$ be the set of all admissible state-action pairs, and let $\mathcal{B}(\mathcal{S})$ be the Borel sigma algebra on \mathcal{S} . Then, the transition probability kernel $T : \mathcal{K} \rightarrow [0, 1]$ is a stochastic kernel on \mathcal{S} specified for every $((\mathbf{x}, r), u) \in \mathcal{K}$ by

$$T(B \mid ((\mathbf{x}, r), u)) = \int_{(\mathbf{y}, s) \in B} \mathbb{I}_{\{s=r\}} dF_n(\mathbf{y} - \mathbf{A}\mathbf{x} - \mathbf{b}u), \quad \forall B \in \mathcal{B}(\mathcal{S}),$$

where F_n is the distribution of the state disturbance.

- The Single Stage Cost is a measurable function $g : \mathcal{K} \rightarrow \mathbb{R}_+$, defined by $g((\mathbf{x}, r), u) = \mathbf{x}^T Q \mathbf{x} \forall (\mathbf{x}, r) \in \mathcal{S}$.
- Discount factor = γ .

The cost of applying π^* to this MDP is the state penalizing cost $J_{sp,r}$. Since π^* is a stationary policy, we invoke the following from [Ber11, Cor. 3.1.1.1].

Proposition 7.2 ([Ber11]). Let μ be a stationary policy for the above MDP. Suppose the single stage cost $g(\mathbf{x}, u) \geq 0, \forall (\mathbf{x}, u) \in \mathcal{S} \times \mathbb{R}$. Then the cost functional $J_\mu(\cdot)$ associated with μ satisfies

$$J_\mu(\mathbf{x}, r) = \mathbf{x}^T Q \mathbf{x} + \gamma \mathbb{E} J_\mu(A\mathbf{x} + \mathbf{b}\mu(\mathbf{x}) + \mathbf{n}, r)$$

This shows that under π^* , $J_{sp,r}$ satisfies

$$J_{sp,r}(\mathbf{x}) = \mathbf{x}^T Q \mathbf{x} + \gamma \mathbb{E}_{\mathbf{n}} J_{sp,r}(A\mathbf{x} + \mathbf{b}u^*(\mathbf{x}) + \mathbf{n}). \quad (33)$$

A substitution argument now shows that $J_{sp,r}(\mathbf{x}) = \mathbf{x}^T S \mathbf{x} + \frac{\gamma}{1-\gamma} \mathbb{E} \mathbf{n}^T S \mathbf{n}$, where the matrix S satisfies (32). \square

7.6 Proof of Prop. 3.5

This proof is similar to that of Prop. 4.4.1 in [Ber95] and proceeds in several steps. Recall that the iteration under study is given by

$$S_{t+1} = Q + \left(\gamma A^T \left[I - \gamma \frac{1}{\gamma \mathbf{b}^T K \mathbf{b} + r} K \mathbf{b} \mathbf{b}^T \right] S_t \left[I - \gamma \frac{1}{\gamma \mathbf{b}^T K \mathbf{b} + r} \mathbf{b} \mathbf{b}^T K \right] A \right), t \geq 0, \quad (34)$$

with S_0 set to any SPSD matrix. We first prove convergence starting with $S_0 = 0_{3 \times 3}$, the latter being the all zeros matrix in $\mathbb{R}^{3 \times 3}$, and then show convergence with an arbitrary initial matrix S_0 . Since this means we'll be dealing with multiple initial conditions for the above iteration, we denote the t^{th} iterate by $S_t(S_0)$ to make explicit the initial condition. So, for example, the iterate beginning with the all zeros matrix will be denoted by $S_t(0_{3 \times 3})$.

Before we begin, notice that under the controllability and observability assumptions, the closed loop (noiseless) system given by

$$\mathbf{x}_{t+1} = A\mathbf{x}_t + \mathbf{b}u_t, t \geq 0 \quad (35)$$

is **stable** [Ber95, Prop. 4.4.1 (b)] in the sense that when

$$u_t = -\gamma \frac{1}{\gamma \mathbf{b}^T K \mathbf{b} + r} \mathbf{b}^T K A \mathbf{x}_t = G \mathbf{x}_t,$$

the matrix

$$D = G + A = \left[I - \gamma \frac{1}{\gamma \mathbf{b}^T K \mathbf{b} + r} \mathbf{b} \mathbf{b}^T K \right] A \quad (36)$$

has all three eigenvalues inside the unit circle. Denote the Jordan decomposition [HJ12, Chap. 3] of D by $D = P^{-1}\Lambda_D P$, and note that the previous remark implies that $\lim_{k \rightarrow \infty} D^k = \lim_{k \rightarrow \infty} \Lambda_D^k = 0_{3 \times 3}$ (again, this is entrywise convergence and hence, in Frobenius norm).

Step 1: Let $S_0 = 0_{3 \times 3}$. Then, $S_t = \sum_{k=0}^{t-1} \gamma^k (D^T)^k Q D^k$, $t \geq 1$. Now consider, for the time being, the problem of applying the $u_t = G\mathbf{x}_t, t \geq 0$ to the system in (35) for exactly t time steps⁷, with single stage cost

$$\begin{aligned} g(\mathbf{x}_k, u_k) &= \mathbf{x}_k^T Q \mathbf{x}_k, \quad 0 \leq k \leq t-1, \\ g(\mathbf{x}_t) &= \mathbf{x}_t^T S_0 \mathbf{x}_t, \end{aligned}$$

and $J_t^\pi(\mathbf{x}_0) = \sum_{k=0}^{t-1} \gamma^k g(\mathbf{x}_k, u_k) + \gamma^t \mathbf{x}_t^T S_0 \mathbf{x}_t$. Then we see that under our policy, $J_t^\pi(\mathbf{x}_0) = \mathbf{x}_0^T S_t (0_{3 \times 3}) \mathbf{x}_0$, which means that $\mathbf{x}^T S_t (0_{3 \times 3}) \mathbf{x} \leq \mathbf{x}^T S_{t+1} (0_{3 \times 3}) \mathbf{x}$, $t \geq 0$, $\mathbf{x} \in \mathbb{R}^3$. So $\mathbf{x}^T S_t (0_{3 \times 3}) \mathbf{x}$ is a nondecreasing sequence.

Under our control policy,

$$\begin{aligned} \mathbf{x}_{t+1} &= D\mathbf{x}_t = P^{-1}\Lambda_D P\mathbf{x}_t, \quad t \geq 0, \\ \Rightarrow \mathbf{y}_{t+1} &= \Lambda_D \mathbf{y}_t, \quad t \geq 0, \\ \Rightarrow \mathbf{y}_t &= \Lambda_D^t \mathbf{y}_0, \quad t \geq 1, \end{aligned}$$

where $\mathbf{y}_t = P\mathbf{x}_t$. So the t stage cost can be rewritten as

$$\begin{aligned} J_t^\pi(\mathbf{x}_0) &= \mathbf{x}_0^T S_t (0_{3 \times 3}) \mathbf{x}_0 \\ &= \sum_{k=0}^{t-1} \gamma^k \mathbf{x}_0^T (D^T)^k Q D^k \mathbf{x}_0 \\ &= \sum_{k=0}^{t-1} \gamma^k \mathbf{y}_0^T (\Lambda_D^T)^k P^{-1} Q P \Lambda_D^k \mathbf{y}_0 \\ &\stackrel{(*)}{\leq} \lambda_{\max}(P^{-1} Q P) \|\mathbf{y}_0\|_2^2 \sum_{k=0}^{t-1} \gamma^k |\lambda_{\max}(\Lambda_D)|^k. \end{aligned}$$

In (*), $\lambda_{\max}(P^{-1} Q P)$ and $\lambda_{\max}(\Lambda_D)$ are the largest eigenvalues (in modulus) of $P^{-1} Q P$ and Λ_D respectively. Since all the eigenvalues of D are within the unit circle, the above sum converges as $t \rightarrow \infty$.

So we now have $\{\mathbf{x}_t^T S_t (0_{3 \times 3}) \mathbf{x}_t\}_{t=0}^\infty$ being a nondecreasing sequence bounded from above, which means that it converges (which is also what the above inequalities show). Hence, beginning with the all zeros matrix, the iteration (34) converges to some limit, say S , that satisfies (15). Using different values for the vector \mathbf{x}_0 , it can be shown that this convergence is in the Frobenius norm.

Step 2: Let S_0 be any arbitrary symmetric positive semidefinite matrix. Going back to the t step finite horizon formulation in Step 1, we see that, modifying the final stage cost to $g(\mathbf{x}_t) = \mathbf{x}_t^T S_0 \mathbf{x}_t$,

$$\mathbf{x}^T S_t(S_0) \mathbf{x} = \underbrace{\mathbf{x} \gamma^t (D^t)^T S_0 D^t}_{T1} + \underbrace{\sum_{k=0}^{t-1} \gamma^k \mathbf{x} (D^T)^k Q D^k \mathbf{x}}_{T2}.$$

In the above equation, $T1 \rightarrow 0$ and we have already shown that $T2$ converges. This completes the proof of convergence of the iterates in (34). Finally, to show uniqueness, assume the contrary, i.e., there exists another S' that is a fixed point of Eqn. (34). Then, beginning (34) with $S_0 = S'$, we see that $S_t(S') \rightarrow S$, which means $S' = S$. Hence, the solution to (15) is unique. \square

⁷This means we're now working with a *finite* horizon version of the problem, with the horizon being t time steps.

7.7 Proof of Thm. 3.6

We first define the norm $\|\cdot\|$ as in Eqn. (12), the space \mathcal{V} and the metric ρ exactly as in the proof of Thm. 3.1. We also note that $\langle \mathcal{V}, \rho \rangle$ is a complete metric space and the set $\mathcal{H} := \{v \in \mathcal{V} : v \text{ is concave nondecreasing}\}$ is closed in \mathcal{V} . Next, recall that $D = \left[I - \frac{1}{\mathbf{b}^T K \mathbf{b} + r} \mathbf{b} \mathbf{b}^T K \right] A$ and define the operator $T_\pi : \mathcal{G} \rightarrow \mathcal{G}$ by

$$T_\pi v(\mathbf{x}, r) = \mathbf{x}^T Q \mathbf{x} + \gamma v(D\mathbf{x}, r). \quad (37)$$

The fact that $v \in \mathcal{V} \Rightarrow T_\pi v \in \mathcal{V}$ follows using the ideas in the proof of Lem. 3.2 and that $v \in \mathcal{H} \Rightarrow T_\pi v \in \mathcal{H}$ from the proof of Lem. 3.3.

Observe that the zero cost function v_0 defined by $v_0(\mathbf{x}, r) = 0, \forall (\mathbf{x}, r) \in \mathcal{S}$ is in \mathcal{H} . So, we now only need to show that, beginning with $v_0, T^k v \rightarrow J_{sp,r}$. This will follow from the proof of Lem. 3.4, if we can show that $\|S_t - S\|_{F \rightarrow 0}$, but that is precisely what Prop. 3.5 states. Hence, $J_{sp,r} \in \mathcal{H}$ which concludes the proof of the theorem. \square

7.8 Proof of Thm. 3.7

We have proved that $\mathcal{E}_\mathbf{x}^*$ is concave nondecreasing in volatility. Basic convex analysis shows that the epigraph of a convex function is always convex [BN03] which, therefore is true of the the region bounded *below* this *concave* curve. Since at optimality the volatility constraint is active, the boundary of \mathcal{C} is achieved by the policy that attains the optimum in (22) which, by Thm 4.2 in [Alt99], exists. This means that, \mathcal{C} , the set of $(\mathcal{E}, \mathcal{V})$ pairs that can be achieved, is a subset of the subset of \mathbb{R}^2 bounded by this curve. Therefore, to complete the proof, we need to show that every point in the region below this curve is achievable.

Recall that at optimality, we require that

$$\mathbf{x}_0 \frac{dK_\lambda}{d\lambda} \mathbf{x}_0 + \frac{\gamma}{1-\gamma} \mathbb{E} \mathbf{n}^T \frac{dK_\lambda}{d\lambda} \mathbf{n} = \alpha, \quad (38)$$

and that $\mathbf{x} \frac{dK_\lambda}{d\lambda} \mathbf{x}$ is decreasing in λ . This means that as volatility $\alpha \downarrow 0$, to satisfy (38) above, $\lambda \uparrow \infty$, which means that $J_r^* \uparrow \infty$ and $\mathcal{E}_r^* \downarrow -\infty$. This means that the capacity region is convex, but **not compact**. Moreover, since \mathcal{E}_r^* is a nonpositive, nodecreasing function of α , it has a limit point. Now, let \mathcal{C}° denote the interior of \mathcal{C} . It is easy to see that for every point $\mathbf{z} = (v, e) \in \mathcal{C}^\circ$, there exist points $\mathbf{z}_1 = (v_1, e_1^*)$ and $\mathbf{z}_2 = (v_2, e_2^*)$ such that $e_i^*, i = 1, 2$ is the optimal efficiency for volatility v_i and $\mathbf{z} = \mu \mathbf{z}_1 + (1-\mu) \mathbf{z}_2$ for some $\mu \in [0, 1]$. We need to show that there exists some admissible policy that achieves (v, e) .

Towards this end consider the policy π_μ defined as follows. Let $\pi_i, i = 1, 2$ be the policy that achieves (v_i, e_i^*) . At time $t = 0$, the policy π_μ chooses π_1 with probability μ and π_2 with probability $1-\mu$ and continues with this choice for all time slots thereafter. The associated expectation operator is $\mathbb{E}_\mathbf{x}^{\pi_\mu}(\cdot) = \mu \mathbb{E}_\mathbf{x}^{\pi_1}(\cdot) + (1-\mu) \mathbb{E}_\mathbf{x}^{\pi_2}(\cdot)$. Such a policy obviously achieves efficiency $\mu e_1^* + (1-\mu) e_2^*$ and volatility $\mu v_1 + (1-\mu) v_2$ (which are both finite), and is therefore also admissible.

7.9 Proof of Prop. 4.1

It is easy to check that the conditions for controllability and observability do not change from the ones in Sec. 2, and therefore, going through the constrained MDP analysis (see Sec. 3.2) once more on this new

system, the optimal cost is given by

$$\begin{aligned} \mathcal{L}_r^{(ren),*}(\mathbf{x}) &= \sup_{\lambda \geq 0} \left(\mathbf{z}^T K_\lambda^{(r)} \mathbf{z} + \frac{\gamma}{1-\gamma} \mathbb{E}(\mathbf{n}^{(r)})^T K_\lambda^{(r)} \mathbf{n}^{(r)} \right. \\ &\quad \left. - \lambda \alpha \right), \quad \forall \mathbf{x}_0 \in \mathbf{R}^3. \end{aligned} \quad (39)$$

As renewable supplies proliferate (a) the aggregate supply from these sources obviously increases and (b) supplied power becomes more volatile. The factor in Eqn. (REN) that captures both of these effects is the renewable supply variance ψ_r . As the contribution of renewables increases, so does ψ_r . Returning to Eqn. (39), notice that the contribution of the state disturbance terms to the optimal cost is $\mathbb{E}(\mathbf{n}^{(r)})^T K_\lambda^{(r)} \mathbf{n}^{(r)}$ (ignoring the constant factor), which can be rewritten as $\mathbb{E}Tr \left(K_\lambda^{(r)} (\mathbf{n}^{(r)})^T \mathbf{n}^{(r)} \right) = Tr \left(K_\lambda^{(r)} \Psi_n^{(r)} \right)$, where $Tr(M)$ is the trace of the matrix M . Since $\Psi_n^{(r)}$ is diagonal, it is clear that as ψ_r increases, so does $Tr \left(K_\lambda^{(r)} \Psi_n^{(r)} \right)$, which increases the optimal cost.

We already know from our analysis in Sec. 3.2 that $\mathcal{L}_r^{(ren),*}(\mathbf{x})$ is nondecreasing in α and hence, when ψ_r increases, the only way to maintain cost, i.e., social utility, the same is to increase α . But by definition, an increase in α automatically implies increased volatility in prices.

7.10 Details of Experiments

The market, as mentioned before, is completely specified by the tuple (A, F_n, Q, r, γ) . Recall that the matrix A is of the form

$$A = \begin{bmatrix} \beta & 0 & -\phi_1 \\ 0 & \sigma & \phi_2 \\ 0 & 0 & 1 \end{bmatrix},$$

where $\beta, \sigma, \phi_1, \phi_2$ are nonnegative reals. In our experiments, we have chosen $\beta = 0.995, \sigma = 0.900, \phi_1 = 0.5, \phi_2 = 0.25$ and the discount factor $\gamma = 0.5$. The controllability matrix turns out to be

$$\begin{bmatrix} 0 & -0.5 & -0.9975 \\ 0 & 0.25 & 0.475 \\ 1 & 1 & 1 \end{bmatrix},$$

which has a rank of 3, and hence, the system is controllable. Since we have performed experiments for multiple values of the control penalty r , these values are specified in the description of each experiment in Sec. 5. The state disturbance is assumed to be IID Gaussian, with 0 mean and covariance matrix

$$\Psi_n = \begin{bmatrix} 2.00 & 0 & 0 \\ 0 & 2.00 & 0 \\ 0 & 0 & 0 \end{bmatrix},$$

so $F_n \equiv \mathbf{N}(\mathbf{0}, \Psi_n)$. With regards to the cost function, to ensure observability, Q was designed to be symmetric positive definite with a minimum eigenvalue of 0.5

$$Q = \begin{bmatrix} 2.38 & -1.73 & -0.15 \\ -1.73 & 2.15 & 0.16 \\ -0.15 & 0.16 & 0.52 \end{bmatrix}.$$

8 Supplementary Material

In Sections 4 and 5 we studied the effect of the presence of large-scale renewable sources (such as wind farms and solar parks) on the *supply* side of our deregulated market. But apart from large-scale renewable generation, the electricity market has recently also witnessed burgeoning power supply local to the demand side or customer side, such as isolated solar panels and small wind turbines. In this section, we would like to report some preliminary results of studying the effect such sources could have on the volatility of real-time electricity prices. These so-called Distributed Energy Resources or DERs [Rob, KDMT16], are generally located “behind the meter,” have nearly zero marginal operating costs [Jos19] and their output is largely unaffected by grid state variables such as the instantaneous price of electricity. Consequently, studying the effect of such sources will require some modification to our original system model in Eqn. (SYS).

To incorporate the aforementioned features of DERs, we propose the following market model. As in Sec. 4, we introduce a new state variable, y_t , that represents DER supply and evolves as

$$y_t = \sigma_{rn} P_{rn}(t) + w_t, \quad (40)$$

where $\sigma_{rn} P_{rn}(t)$ represents the contribution of the nominal output of the DERs to the aggregate market demand, and $(w_t)_{t=0}^{\infty}$ is a sequence of zero-mean independent, identically distributed random variables that models random temporal variability (caused by weather conditions, etc.). In contrast to earlier notation, we denote the variance of w_t by ψ_w . To account for the fact that this portion of the load is being handled at the consumer end, the market demand evolution needs to be modified to

$$d_{t+1} = (\beta d_t - \phi_1 p_t - y_t)^+, \quad (41)$$

where for any $x \in \mathbb{R}$, $(x)^+ = \max(x, 0)$. Notice that, in the absence of the DER contribution term y_t , Eqn. 41 boils down to our original demand equation in (SYS).

Nominal renewable generation (especially through photovoltaic sources) tends to show a step-like behavior over a period of $T = 24$ hours, peaking around midday. As empirical data from the California ISO shows [ISO], renewable supply satisfies approximately 10% of the total demand over about 14 hours and approximately 44% for during the other 10, and we model this by setting

$$P_{rn}(t) = \begin{cases} v_1, & \text{if } t < 0.3T \text{ or } t > 0.7T \\ v_2, & \text{if } t \in [0.3T, 0.7T] \end{cases}, \quad (\dagger)$$

Further, it has been observed that apart from the current demand, the price of electricity is also dependent on load *fluctuations* [WMO14]. We therefore modify the price evolution equation in (SYS) to reflect this observation as follows

$$p_{t+1} = p_t + u_t + \mathcal{D}(d_t, d_{t+1}), \quad (42)$$

where, as in [WMO14], the function $\mathcal{D}(\cdot, \cdot) : \mathbb{R}^2 \rightarrow \mathbb{R}_+$ is assumed to be jointly convex in its arguments and monotonically increasing in the absolute value of the difference in demand, i.e., if $|x - y| > |x' - y'|$ then $\mathcal{D}(x, y) > \mathcal{D}(x', y')$.

We now illustrate what happens when an RTO or an ISO, oblivious to the presence of demand-side renewable supply, decides to employ the optimal control policy discussed in Sec. 2 on this market. In Fig. 11, we plot the increase in price volatility with increasing renewable supply. Recall that the variance of the state disturbance for the supply process was denoted by ψ_s , and let $\Delta = \frac{\psi_w}{\psi_w + \psi_s}$ represent the fraction of renewable supply in the market. Fig. 11 now shows how market price shows unbounded variability as Δ increases to 100% of the market share. We choose

$$\mathcal{D}(d_t, d_{t+1}) := \xi(d_t - d_{t+1})^2 \quad (43)$$

to model price variations due to demand fluctuations. The rest of the parameters of the market are as given in Sec. 7.10. The figure shows that volatility increases to unacceptable levels even for moderately small values of ξ . This rather precipitous increase in volatility is why we choose to term this phenomenon a “[volatility cliff](#),” since, beyond a certain level of Δ , the variability rise is high enough to force the dispatch of additional *controllable* power supplies, such as coal or natural gas, to reduce Δ and hence, volatility.

Price fluctuations in real time electricity markets have been observed and reported in, for example, the New England ISO [KR00] *before* renewable proliferation became significant. But the volatility reported therein (see the section titled “Price Volatility” in [KR00, Pg. 5]), is much smaller than that predicted by our model. This suggests that renewable supplies on the demand side, especially intermittent photovoltaic and wind sources, could be harmful to deregulated power markets if adopted without due consideration.

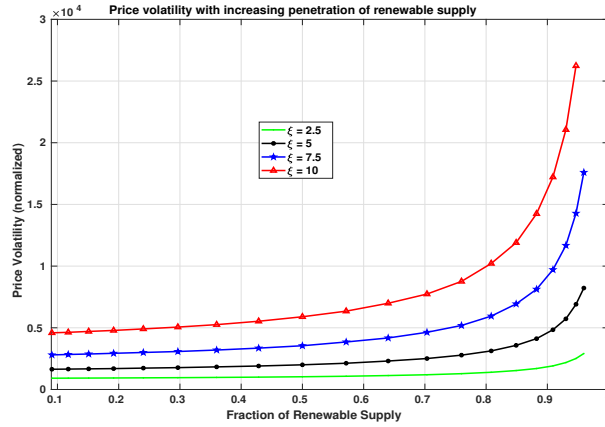


Figure 11: The rapid increase of market price volatility with increasing demand-side renewable penetration. We used $\sigma_{rn} = 1.00$, and in Eqn.(†), we set $v_1 = 0.1$ and $v_2 = 0.44$. The initial condition $\mathbf{x}_0 = [1, 1, 2]^T$. The other parameters of the market are specified in Sec. 7.10 in the Appendix.